BIOCHEMISTRY
including biophysical chemistry & molecular biology

Article

pubs.acs.org/biochemistry

Interaction of Antimicrobial Peptide Magainin 2 with Gangliosides as a Target for Human Cell Binding

Yu Miyazaki, Megumi Aoki, Yoshiaki Yano, and Katsumi Matsuzaki*

Graduate School of Pharmaceutical Sciences, Kyoto University, 46-29 Yoshida-Shimoadachi-cho, Sakyo-ku, Kyoto 606-8501, Japan

ABSTRACT: Understanding how antimicrobial peptides (AMPs) interact with human cells is important to the development of antimicrobial agents as well as anticancer drugs. However, little is known about the mechanisms by which AMPs bind to cells and exert cytotoxicity. Negatively charged gangliosides on the cell surface are a potential target for cell binding. In this study, we investigated the interaction of F5W-magainin 2 (MG) with gangliosides in detail. MG was colocalized with gangliosides on HeLa cells, indicating that gangliosides act as a receptor for MG. MG also bound to gangliosides in model membranes. The affinity increased with the number of negatively charged sialic acid residues. Physicochemical studies revealed that MG interacts with the monosialoganglioside GM1 differently from the typical bacterial anionic phospholipid phosphatidylglycerol. MG bound to GM1 more strongly than to phosphatidylglycerol, and the binding isotherm for GM1 could be analyzed by the Langmuir equation assuming charge neutralization. This is in contrast to the binding of AMPs to phosphatidylglycerol-containing bilayers, which has been described by the electrostatic attraction−surface partitioning model. Fluorescence resonance energy transfer experiments supported the clustering of GM1, but not phosphatidylglycerol, by MG. Quenching data suggested that MG is bound to the sugar region of GM1. The bound peptide assumed a helical structure and induced the leakage of calcein and the coupled flip-flop of lipids, indicating the peptide also forms a toroidal pore in GM1-containing vesicles. However, the membrane permeabilizing activity was weaker against GM1-containing membranes than phosphatidylglycerol-doped liposomes in accordance with the trapping of the peptide in the sugar region. These results shed light on AMP−human cell interaction.

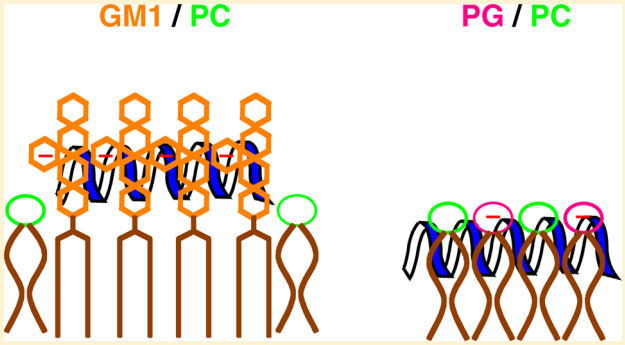

More than 1200 antimicrobial peptides (AMPs) have been discovered in plants, insects, and vertebrates, including humans, constituting host defense systems against invading pathogenic microorganisms.[1−4] Many attempts have been made to utilize AMPs as antibiotics, because they exhibit a broad spectrum of antimicrobial activity and do not easily induce resistance compared to conventional antibiotics. Furthermore, AMPs are promising seeds for anticancer therapy.[5,6] Therefore, understanding how AMPs interact with human cells, both normal and cancerous, is important to the development of effective antimicrobial agents and anticancer drugs. However, little is known about the mechanisms by which AMPs bind to cells and exert cytotoxic effects.

Polycationic AMPs are more toxic to bacterial cells than to mammalian cells mainly because the former are more negatively charged.[1,7,8] The cell membranes of bacteria are rich in acidic phospholipids, such as phosphatidylglycerol and cardiolipin. The cell walls also contain anionic molecules, such as lipopolysaccharides in the outer membrane of Gram-negative bacteria and teichoic acids and lipoteichoic acids in the peptidoglycan of Gram-positive bacteria. In contrast, the outer leaflets of mammalian plasma membranes are mainly composed of zwitterionic phosphatidylcholine and sphingomyelin.

Several anionic molecules on the surface of mammalian cells have been suggested to serve as a molecular portal for the cellular interaction of AMPs.[5,6] These molecules, including phosphatidylserine (PS),[9] heparan sulfate proteoglycan glypican-1,[10] and sialylated truncated mucin O-glycans,[11] are strongly expressed in tumor cells, although their interaction with AMPs has been investigated little.[12]

In this study, we focus on negatively charged sphigoglycolipid gangliosides as a target for human cell binding and investigate in detail their interaction with the archetypical AMP F5W-magainin 2 (MG) in comparison with the typical bacterial anionic lipid phosphatidylglycerol. We find that gangliosides are targets for MG on human cells but MG interacts with them in a manner different from that of phosphatidylglycerol.

MATERIALS AND METHODS

Materials. MG (GIGKWLHSAKKFGKAFVGEIMNS) and TMR-MG (MG labeled with tetramethylrhodamine at the N-terminus) were synthesized by a standard fluoren-9-ylmethoxycarbonyl-based solid phase method, as described previ-

Received: October 30, 2012
Revised: November 28, 2012
Published: November 29, 2012

dx.doi.org/10.1021/bi301470h | *Biochemistry* 2012, 51, 10229−10235

ously.[13,14] The synthesized peptides were identified by ion spray mass spectroscopy, and their purity (>95%) was determined by analytical reverse phase high-performance liquid chromatography. Egg yolk L-α-phosphatidylcholine (PC), 1,2-dipalmitoyl-*sn*-glycero-3-phosphocholine (DPPC), L-α-phosphatidyl-DL-glycerol enzymatically converted from PC (PG), bovine brain gangliosides [monosialoganglioside GM1 (GM1), disialoganglioside GD1a (GD1a), disialoganglioside GD1b (GD1b), and trisialoganglioside GT1b (GT1b)], and pyrene-labeled GM1 (Pyr-GM1) were purchased from Sigma (St. Louis, MO). 1-Hexadecanoyl-2-(1-pyrenedecanoyl)-*sn*-glycero-3-phosphocholine (Pyr-PC), 1-hexadecanoyl-2-(1-pyrenedecanoyl)-*sn*-glycero-3-phosphoglycerol (Pyr-PG), and 1-palmitoyl-2-{6-[(7-nitrobenz-2-oxa-1,3-diazol-4-yl)amino]caproyl}-L-α-phosphatidylcholine (NBD-PC) were obtained from Invitrogen (Eugene, OR). 1-Palmitoyl-2-stearoyl(5-doxyl)-L-α-phosphatidylcholine (5-doxyl-PC) and 1-palmitoyl-2-stearoyl(12-doxyl)-L-α-phosphatidylcholine (12-doxyl-PC) were purchased from Avanti Polar Lipids (Alabaster, AL).

Lipid Vesicles. Large unilamellar vesicles (LUVs) were prepared and characterized as described elsewhere.[15] Briefly, a lipid film, after drying under vacuum overnight, was hydrated with a Tris buffer [10 mM Tris, 150 mM NaF, and 1 mM EDTA (pH 7.4)] or a calcein solution [70 mM calcein and 1 mM EDTA (pH 7.4)] for leakage experiments and vortex-mixed to produce multilamellar vesicles. NaF was used to reduce UV absorption by buffer components and thus to improve the signal-to-noise ratio for circular dichroism (CD) measurements.[16] The suspension was subjected to five freeze–thaw cycles and then extruded through polycarbonate filters (100 nm pore size filter, 21 times). The lipid concentration was determined in triplicate by phosphorus analysis for phospholipids[17] or the resorcinol–hydrochloric acid method for gangliosides.[18]

CD Spectra. CD spectra of 25 μM MG in the absence and presence of LUVs were measured on a Jasco J-820 apparatus at 37 °C, using a 1 mm path length quartz cell to minimize the absorbance due to buffer components. We confirmed that the light scattering due to a high concentration of LUVs did not distort the spectrum.[19] The instrumental outputs were calibrated with nonhygroscopic ammonium *d*-camphor-10-sulfonate.[20] Sixteen scans were averaged for each sample. The blank spectra (LUV suspension or buffer) were subtracted.

Binding. The binding of the peptide to LUVs was estimated on the basis of its Trp fluorescence. Peptide solutions (2 μM) were titrated with a vesicle suspension, while the fluorescence spectra of the Trp residue were recorded at an excitation wavelength of 280 nm on a Shimadzu (Kyoto, Japan) RF-5300 spectrofluorometer. Blank spectra (LUVs) were subtracted, and volume correction for dilution (up to 5%) was conducted.

Leakage. The membrane permeabilizing activity was estimated by calcein leakage.[13] Calcein-free LUVs were mixed with LUVs containing calcein to obtain the desired lipid concentration. The release of calcein from the LUVs was fluorometrically monitored at an excitation wavelength of 490 nm and an emission wavelength of 520 nm. The maximal fluorescence intensity corresponding to 100% leakage was determined by addition of 10% Triton X-100 (20 μL) to the sample (2 mL). The apparent percent leakage value was calculated according to

$$\%\text{apparent leakage} = 100(F - F_0)/(F_t - F_0) \quad (1)$$

where F and F_t denote the fluorescence before and after addition of the detergent, respectively and F_0 represents the fluorescence of the intact vesicles.

Fluorescence Resonance Energy Transfer (FRET). MG (2 μM) was mixed with LUVs with and without 1 mol % Pyr-GM1, Pyr-PC, or Pyr-PG as an acceptor, and fluorescence spectra were recorded at an excitation wavelength of 280 nm. The FRET efficiency E was calculated as

$$E = 1 - F/F_0 \quad (2)$$

where F and F_0 represent the fluorescence intensity at 336 nm in the presence and absence of the acceptor, respectively, after the subtraction of blank spectra and correction for inner filter effects[21] due to light absorption by the pyrene chromophore at 336 nm.

Quenching. MG (2 μM) was mixed with LUVs with 10 mol % 5-doxyl-PC or 12-doxyl-PC, and fluorescence spectra were recorded at an excitation wavelength of 280 nm. The concentration of actual spin-labeled lipid in each doxyl-PC had been determined on the basis of the quenching of NBD-PC fluorescence.[22] The distance between the bilayer center and the Trp residue (z_{CF}) was estimated according to the parallax method.[22]

$$z_{CF} = -\frac{1}{2L_{5-12}}\left[\frac{1}{\pi C}\ln\left(\frac{F_5}{F_{12}}\right) + L_{5-12}^2\right] + L_{c-5} \quad (3)$$

where C is the two-dimensional concentration of the quencher in the membrane (0.0014 molecule/Å^2, assuming that the cross section of a lipid molecule is 70 Å^2), F_5 and F_{12} denote the fluorescence intensities measured in duplicate in the presence of 5-doxyl-PC and 12-doxyl-PC, respectively, and L_{5-12} (6.3 Å) and L_{c-5} (12.15 Å) represent the vertical lengths from the doxyl group of 5-doxyl-PC to that of 12-doxyl-PC and the bilayer center, respectively.[22]

Lipid Flip-Flop. The peptide-induced lipid flip-flop was assessed as previously reported.[15] LUVs doped with 1.5 mol % NBD-PC were mixed with 1 M sodium dithionite and 1 M Tris (10 mM lipid and 70 mM dithionite) and incubated for 15 min at 30 °C to produce inner leaflet-labeled vesicles. The vesicles were immediately separated from dithionite by gel filtration. The asymmetrically NBD-labeled LUVs (2 mL) were incubated with or without the peptide for various periods at 37 °C. The fraction of NBD-lipids that had flopped during incubation was measured on the basis of fluorescence quenching by sodium dithionite. After the reaction with 20 μL of 5 mg/mL trypsin for 2 min to recover the barrier, 20 μL of a 1 M sodium dithionite/1 M Tris solution was added. Fluorescence was monitored at excitation and emission wavelengths of 460 and 530 nm, respectively.

Confocal Microscopy. Human cervical carcinoma HeLa cells were cultured in Eagle's minimum essential medium (Sigma) with 10% heat-inactivated fetal bovine serum, 50 units/mL penicillin, and 50 μg/mL streptomycin in a humidified incubator at 37 °C and 5% CO_2. The cells were seeded (100000 cells/dish) on a 35 mm glass bottom dish (catalog no. 3910-035, IWAKI, Tokyo, Japan) and incubated for 24 h before being stained and observed. After removal of the culture medium, MG (24.4 μM) and TAMRA-MG (0.6 μM), dissolved in 1 mL of PBS(+) [137 mM NaCl, 8.1 mM Na_2HPO_4, 2.68 mM KCl, 1.47 mM KH_2PO_4, 0.9 mM $CaCl_2$, and 0.33 mM $MgCl_2$ (pH 7.4)], were applied to the cells. After incubation for 30 min, the cells were washed with PBS(+),

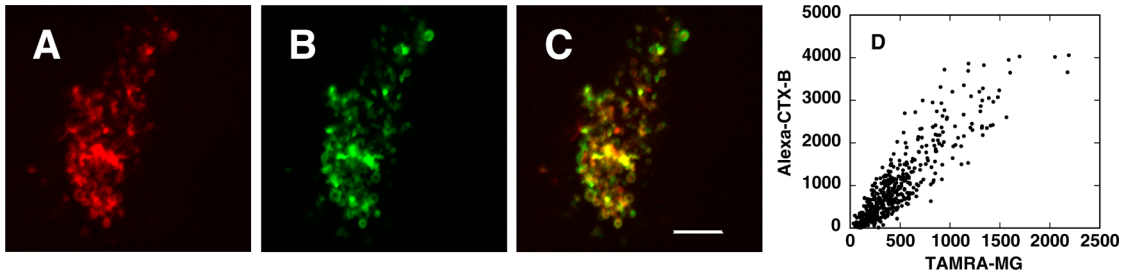

Figure 1. Colocalization of MG with gangliosides on HeLa cells. HeLa cells (10^5 cells) were incubated with a mixture of TAMRA-MG (0.6 μM) and unlabeled MG (24.4 μM) for 30 min. After being washed with PBS, gangliosides were stained with 5 μg/mL Alexa Fluor 488-labeled CTX-B. The cells were washed and observed on a C1si confocal laser scanning microscope from Nikon. The focal plane was close to the cell surface. TAMRA, Alexa Fluor 488, and merged images are shown in panels A–C, respectively. The bar represents 10 μm. (D) Fluorescence intensity of TAMRA (abscissa) and Alexa Fluor 488 (ordinate) plotted for each pixel.

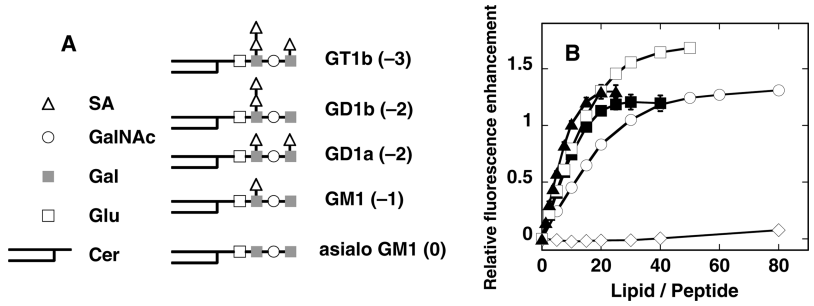

Figure 2. Binding of MG to various ganglioside-containing liposomes. (A) Schematic representation of the structure of the gangliosides used. SA, sialic acid; GalNAc, *N*-acetylgalactosamine; Gal, galactose; Glu, glucose; Cer, ceramide. The number in parentheses indicates the net charge at neutral pH. (B) The MG (2 μM) solution was titrated with LUVs composed of ganglioside and PC (3:7) at 37 °C. The relative enhancement of Trp fluorescence at 336 nm (excited at 280 nm) is plotted as a function of L:P. The experiments were performed in duplicate, and the error bars denote standard deviations. Gangliosides: (◇) asialo GM1, (○) GM1, (■) GD1a, (□) GD1b, and (▲) GT1b.

stained with 5 mg/mL cholera toxin subunit B (CTX-B) labeled with Alexa Fluor 488 (Life Technologies, Carlsbad, CA) for 15 min, and again washed with PBS(+). Live-cell images for TAMRA and Alexa Fluor 488 were obtained with a confocal microscope (C1si, Nikon, Tokyo, Japan).

RESULTS

Binding of MG to Gangliosides. The binding of MG to gangliosides was investigated in both living cells and model membranes. TMR-MG mixed with MG was incubated with HeLa cells for 30 min, and surface gangliosides were visualized with Alexa Fluor 488-labeled CTX-B. CTX-B binds to not only GM1 but also GD1b and their fucosylated species.[23,24] As Figure 1 shows, TMR-MG was colocalized with gangliosides. Anionic PS has been shown to act as a binding site for AMPs.[12] Therefore, the surface expression of PS was examined with Alexa Fluor 488-labeled annexin V. No detectable staining was observed, indicating that the contribution of PS to the binding of MG was negligible (data not shown).

MG interacted also with gangliosides in lipid bilayers. The binding of MG to gangliosides was assessed on the basis of Trp fluorescence. The MG solution was titrated with PC liposomes containing various gangliosides at 30 mol %.[a] The structures of gangliosides used are summarized in Figure 2A. The binding induced an enhancement of fluorescence intensity and a blue shift of the wavelength of maximal intensity. The relative increase in fluorescence at 336 nm is plotted as a function of the lipid-to-peptide molar ratio, L:P (Figure 2B). The affinities (the L:P value giving 50% of the maximal intensity change) were in the following order: asialo GM1 ≪ GM1 < GD1b ≤ GD1a < GT1b (indicating that negative charges due to sialic acid residues play a crucial role in binding).

Binding Affinity for GM1 versus That for PG. We systematically compared the interaction of MG with GM1 and PG, both having one negative charge, to characterize MG–ganglioside interaction. The binding affinity of MG for GM1/PC LUVs (3:7) was significantly greater than that for PG/PC LUVs (3:7) despite a similar membrane charge density (Figure 3A). Binding isotherms (Figure 3B) were obtained from Figure 3A as reported elsewhere[25] and analyzed using the conventional Langmuir equation.

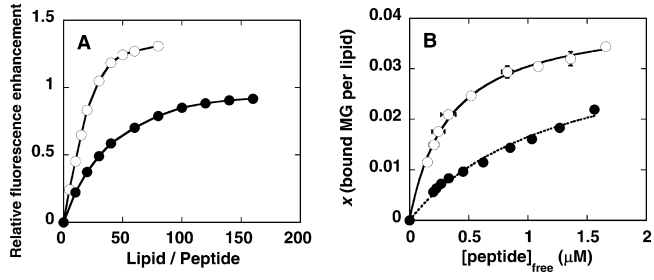

Figure 3. Comparison of binding of MG to GM1 and PG. The MG (2 μM) solution was titrated with LUVs composed of GM1 and PC (3:7) (○) or PG and PC (3:7) (●) at 37 °C. The experiments were performed in duplicate, and the error bars denote standard deviations. (A) Relative enhancement of Trp fluorescence at 336 nm plotted as a function of L:P. (B) Binding isotherms obtained from panel A. The traces are the best fit binding isotherms using eq 4 and the parameters described in the text.

dx.doi.org/10.1021/bi301470h | *Biochemistry* 2012, 51, 10229–10235

$$x = \frac{x_{max} K[\text{peptide}]_{free}}{1 + K[\text{peptide}]_{free}} \quad (4)$$

where x denotes the number of bound peptides per lipid, x_{max} is its maximal value, and K and $[\text{peptide}]_{free}$ represent the binding constant and the free peptide concentration, respectively. The best fit parameters were as follows: $K = (2.92 \pm 0.18) \times 10^6$ M^{-1} and $x_{max} = 0.0408 \pm 0.0008$ for GM1/PC LUVs, and $K = (0.76 \pm 0.13) \times 10^6$ M^{-1} and $x_{max} = 0.0382 \pm 0.0039$ for PG/PC LUVs.

Secondary Structure in GM1 versus That in PG. The difference in binding affinity may be related to a difference in the conformation of the membrane-bound peptide. The secondary structure of membrane-bound MG was estimated by CD spectra. CD spectra of 25 μM MG were measured in the presence of saturating concentrations of GM1/PC and PG/PC vesicles (Figure 4). The spectra, although noisy because of high concentrations of lipids (2–4 mM), were characterized by double minima around 208 and 222 nm, indicating the formation of α-helical structures.[16] The $[\theta]_{222}$ value for GM1/PC LUVs at an L:P of 80 (99% bound as calculated from eq 4) was −19800 deg cm^2 dmol^{-1} (helicity of 57.6%[26]), slightly more negative than the value (−16200 deg cm^2 dmol^{-1}, helicity of 45.7%) for PG/PC LUVs at an L:P of 160 (99% bound).

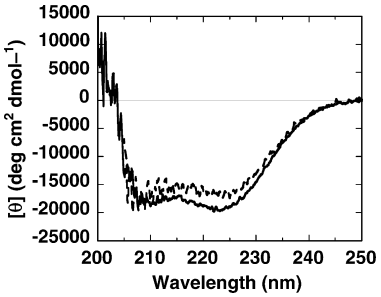

Figure 4. CD spectra of membrane-bound MG at 37 °C. CD spectra of 25 μM MG were measured in the presence of GM1/PC (—) and PG/PC (---) LUVs at L:P values of 80 and 160, respectively.

Binding Specificity for GM1 versus That for PG. The difference in binding affinity may also result from a difference in specificity. We, therefore, determined binding specificity using FRET from the Trp residue to the pyrene group attached to each lipid species under completely membrane-bound conditions (Figure 5). In the case of GM1/PC bilayers, a significantly greater FRET efficiency of 35.1% was observed for GM1-labeled vesicles (29:1:70 GM1:Pyr-GM1:PC) than for PC-labeled vesicles (30:69:1 GM1:PC:Pyr-PC; E = 16.7%). This was not caused by a clustering of GM1 because GM1 molecules have been confirmed to be randomly distributed in GM1/PC bilayers.[25] In striking contrast, in the case of PG/PC membranes, similar E values were obtained for 29:1:70 PG/Pyr-PG/PC vesicles (28.9%) and 30:69:1 PG/PC/Pyr-PC vesicles (27.6%). These results strongly suggest that MG specifically interacts with GM1, but not with PG.

Penetration Depth in GM1 versus That in PG. To precisely estimate the depth to which MG penetrates lipid bilayers, we performed fluorescence quenching experiments using 5- and 12-doxyl-PCs under completely membrane-bound conditions. The transversal distances between the bilayer center and the Trp residue (z_{CF}) calculated from eq 3 were 17.3 ± 0.4 and 11.1 ± 0.7 Å for 3:1:6 GM1/doxyl-PC/PC (L:P = 80) and 3:1:6 PG/doxyl-PC/PC (L:P = 160) LUVs, respectively.

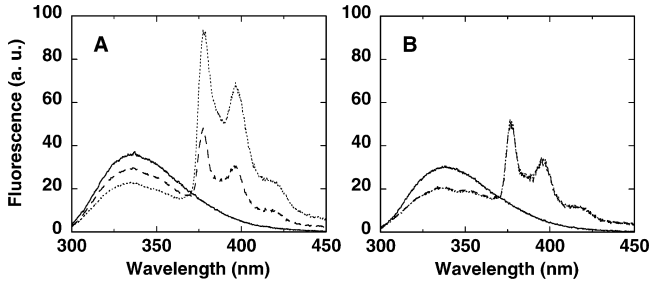

Figure 5. FRET from the Trp residue of MG to pyrene-labeled lipids. The MG (2 μM) solution was mixed with (A) GM1/PC (3:7) or (B) PG/PC (3:7) LUVs without (—) or with (··· and ---) 1 mol % pyrene-labeded lipid, and fluorescence spectra were measured at an excitation wavelength of 280 nm at 37 °C. Pyrene-labeled lipid: (A) Py-GM1 (···) and Py-PC (---) or (B) Py-PG (···) and Py-PC (---).

Leakage against GM1 versus That against PG. The membrane permeabilizing activity of MG was evaluated by conducting calcein leakage experiments. The percent leakage values after 10 min are plotted as a function of L:P in Figure 6.

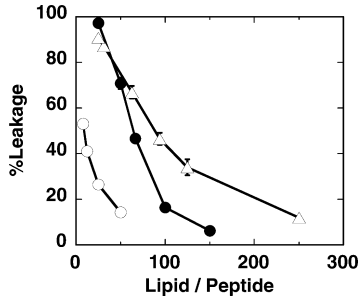

Figure 6. Membrane permeabilizing activity of MG. Percent leakage values of calcein entrapped within LUVs composed of GM1 and PC (3:7) (○), PG and PC (3:7) (●), or DPPG and PG (3:7) (△) after a 10 min incubation at 37 °C plotted as a function of L:P. The lipid concentrations were 50 μM. The experiments were performed in duplicate, and error bars denote standard deviations.

PG/PC membranes were more susceptible to the peptide; 50% leakage was observed at around L:P = 60. In contrast, 6-fold more peptide molecules were required to induce a similar extent of leakage against GM1/PC liposomes. This difference may originate from a difference in membrane fluidity; GM1 with a gel-to-liquid crystalline phase transition temperature of ~37 °C is more rigid than PG with unsaturated acyl chains. To test this possibility, we examined leakage activity against DPPG/PC liposomes. The more rigid DPPG/PC bilayers were not less susceptible to MG than PG/PC membranes.

Toroidal Pore Formation in GM1 versus That in PG. The difference in leakage between GM1- and PG-containing membranes described above may suggest different modes of leakage. MG is known to form a toroidal pore in PG-based membranes, inducing the flip-flop of lipids coupled to leakage.[15] Thus, coupling between leakage and flip-flop was examined. As shown in Figure 7, coupling was observed for both GM1/PC and PG/PC liposomes, indicating that MG forms a toroidal pore in both types of bilayers.

dx.doi.org/10.1021/bi301470h | Biochemistry 2012, 51, 10229–10235

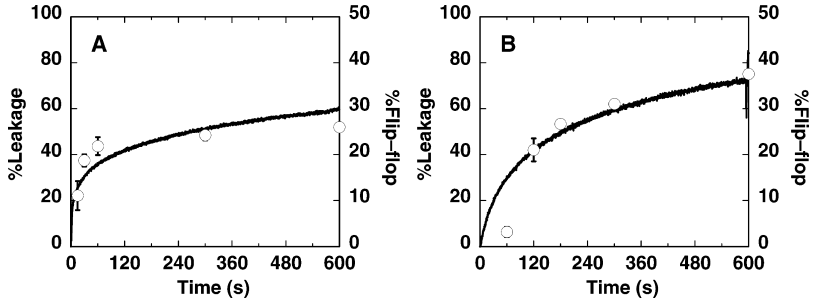

Figure 7. Coupling between dye leakage and lipid flip-flop induced by MG at 37 °C. Time courses of calcein leakage and lipid flip-flop are shown with traces and symbols, respectively, for (A) GM1/PC (3:7) and (B) PG/PC (3:7) vesicles. In the flip-flop experiments, 1.5 mol % C_6-NBD-PC was included. The peptide and lipid concentrations were 6.25 and 50 μM (L:P = 8) in panel A and 1 and 50 μM (L:P = 50) in panel B, respectively.

DISCUSSION

Gangliosides are glycosphingolipids existing on the surface of mammalian cells, especially neurons, and clustered gangliosides have been shown to interact with Alzheimer's amyloid β-peptides.[27] Because of their anionic nature, this class of lipids is expected to interact with cationic peptides, including AMPs. However, little is known about AMP−ganglioside interactions. Lee et al. reported that treatments with an inhibitor of ganglioside synthesis or sialidase rescued tumor cells from cell death induced by the AMP buforin IIb, suggesting that anionic sialic acid residues of gangliosides are involved in the cytotoxicity of the peptide.[28] Here we investigated the interaction of one of the best-studied AMPs, MG, with gangliosides, especially GM1, in detail for the first time and found that MG interacts with GM1 in a manner different from that of the bacterial anionic lipid PG.

The binding of AMPs to PG-containing membranes has been described by the electrostatic concentration−partitioning model,[29,30] although binding isotherms can be phenomenologically described by the Langmuir equation (see the dotted line in Figure 3B).[31] The uniformly distributed negative charges on the membrane give a negative surface potential ϕ_0 according to the Gouy−Chapman theory. Positively charged peptides are electrostatically concentrated immediately above the membrane surface by the Bolztmann factor $\exp(-ze\phi_0/kT)$. z, e, k, and T denote the effective charge of the peptide, the elementary charge, the Bolztmann constant, and the absolute temperature, respectively. The locally concentrated peptides partition into the membrane. A basic assumption of this theory is that PG molecules provide a negative charge density only on the membrane rather than forming a specific peptide−PG complex, the latter being the basis for the Langmuir equation. Our FRET experiments (Figure 5B) clearly showed that MG interacts equally with PG and PC. The observed E values (~28%) correspond to that expected for random FRET.[b,32] A ^{2}H NMR study revealed that the cationic peptide melittin also interacts indistinguishably with PG and PC in mixed bilayers in the presence of 100 mM NaCl, which was comparable with our conditions.[33]

In contrast, MG predominantly interacts with GM1 in GM1/PC bilayers (Figure 5A). Therefore, the binding isotherm can be reasonably analyzed by the Langmuir equation (solid line in Figure 3B). An x_{max} value of 0.0408 corresponds to one peptide molecule per 3.68 GM1 molecules assuming that only the outer leaflet is available to the peptide. Charge neutralization appears to be one of the driving forces for binding because the net charge of MG at pH 7.4 is between +3 and +4. This conclusion is supported by the observations that (1) the binding is mainly determined by the number of sialic acid residues (Figure 2B) and (2) the peptide is trapped in the sugar region of GM1 (vide infra).

The (apparent) binding constant for PG/PC bilayers was smaller than that for GM1/PC bilayers partly because the negative charge of PG is partially masked by the binding of Na^+ to the phosphate group.[34] Another reason is the larger helicity of MG bound to GM1-containing membranes (Figure 4). Our previous study suggested that electrostatic repulsion between the negatively charged C-terminal part of MG containing E19 and the anionic membrane shortens the helix.[35] The C-terminal part experiences less local negative potential in GM1/PC bilayers, in which negative charges of GM1 are masked by positive charges of MG through preferential interaction.

MG formed a toroidal pore also in GM1-based bilayers, although larger amounts of peptides were needed than in PG-containing membranes (Figures 6 and 7). This difference in membrane permeabilizing activity is not due to a difference in the bulk fluidity of membranes (Figure 6). A major driving force of pore formation has been proposed to be membrane thinning effects imposed by AMPs.[36] MG is shallowly inserted into the hydrophobic core of the PG/PC bilayer (z_{CF} = 11.1 Å),[13] inducing a membrane thinning.[37] On the other hand, the peptide trapped in the sugar region of GM1 (z_{CF} = 17.3 Å) cannot effectively thin the membrane. The location of MG in GM1/PC bilayers also supports the conclusion that the peptide specifically interacts with the sialic acid residue of GM1 through electrostatic interaction.

CONCLUSION

Interactions of MG with GM1/PC and PG/PC bilayers are schematically illustrated in Figure 8. MG specifically binds to the sugar region of GM1 (sialic acid residues) in a stoichiometric manner (~1:4), forming an amphipathic α-helix. In contrast, there is no selectivity between PG and PC in PG/PC bilayers, PG merely electrostatically concentrating MG immediately above the membrane. MG partitions into the shallow hydrophobic region, effectively inducing membrane thinning and forming a toroidal pore. The pore formation in GM1/PC bilayers is much less effective because the peptide is trapped far above the hydrophobic region.

This study reveals the specific interaction of MG with gangliosides both in cells and in model membranes. These results will be useful for understanding the interaction of AMPs with human cells and developing antimicrobial or anticancer peptides.

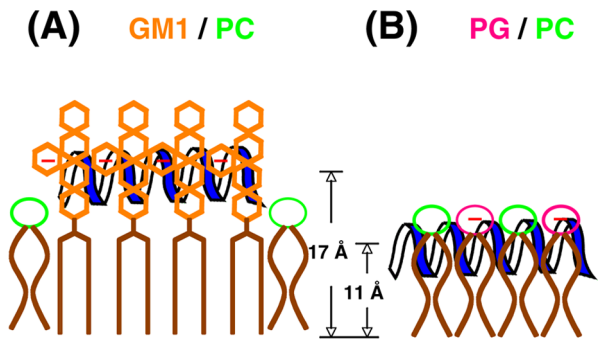

Figure 8. Comparisons between MG−GM1/PC and MG−PG/PC interactions. (A) In GM1/PC membranes, MG selectively binds to GM1 in a stoichiometric manner (∼1:4) and is located in the sugar region. (B) MG is electrostatically concentrated above the PG/PC membrane and partitioned into the shallow hydrophobic region. There is no selectivity between PG and PC interaction in the bilayer phase. Because of the different binding modes, MG forms a toroidal pore more effectively in PG/PC than in GM1/PC bilayers.

AUTHOR INFORMATION

Corresponding Author

*Phone: +81 75-753-4521. Fax: +81 75-753-4578. E-mail: mkatsumi@pharm.kyoto-u.ac.jp.

Funding

This work was supported in part by The Research Funding for Longevity Sciences (22-14) from the National Center for Geriatrics and Gerontology (NCGG), Japan.

Notes

The authors declare no competing financial interest.

ABBREVIATIONS

AMPs, antimicrobial peptides; CD, circular dichroism; CTX-B, cholera toxin subunit B; 5-doxyl-PC, 1-palmitoyl-2-stearoyl(5-doxyl)-L-α-phosphatidylcholine; 12-doxyl-PC, 1-palmitoyl-2-stearoyl(12-doxyl)-L-α-phosphatidylcholine; DPPC, 1,2-dipalmitoyl-*sn*-glycero-3-phosphocholine; FRET, fluorescence resonance energy transfer; GD1a, disialoganglioside GD1a; GD1b, disialoganglioside GD1b; GM1, monosialoganglioside GM1; GT1b, trisialoganglioside GT1b; MG, F5W-magainin 2; LUVs, large unilamellar vesicles; L:P, lipid-to-peptide molar ratio; NBD-PC, 1-palmitoyl-2-{6-[(7-nitrobenz-2-oxa-1,3-diazol-4-yl)amino]caproyl}-L-α-phosphatidylcholine; PC, egg yolk L-α-phosphatidylcholine; PS, phosphatidylserine; PG, L-α-phosphatidyl-DL-glycerol enzymatically converted from PC; Pyr-GM1, pyrene-labeled monosialoganglioside GM1; Pyr-PC, 1-hexadecanoyl-2-(1-pyrenedecanoyl)-*sn*-glycero-3-phosphocholine; Pyr-PG, 1-hexadecanoyl-2-(1-pyrenedecanoyl)-*sn*-glycero-3-phosphoglycerol; TAMRA, tetramethylrhodamine.

ADDITIONAL NOTES

[a]The content of GM1 was limited to 30 mol % to avoid a destabilization of bilayers at higher levels of GM1, which alone forms micelles.

[b]The Förster distance R_0 of the Trp−pyrene pair is 28 Å.[21] One mole percent of the spin-label corresponds to a two-dimensional concentration of 0.112 molecule per R_0^2. Assuming a shortest distance of $0.5R_0$ between the donor and the acceptor, an E value of 28% is estimated for random FRET according to the method of Wolber and Hudson.[32]

REFERENCES

(1) Zasloff, M. (2002) Antimicrobial peptides of multicellular organisms. *Nature 415*, 389−395.

(2) Brown, K. L., and Hancock, R. E. (2006) Cationic host defense (antimicrobial) peptides. *Curr. Opin. Immunol. 18*, 24−30.

(3) Hancock, R. E. W., and Sahl, H.-G. (2006) Antimicrobial and host-defense peptides as new anti-infective therapeutic strategies. *Nat. Biotechnol. 24*, 1551−1557.

(4) Nakatsuji, T., and Gallo, R. L. (2012) Antimicrobial peptides: Old molecules with new ideas. *J. Invest. Dermatol. 132*, 887−895.

(5) Papo, N., and Shai, Y. (2005) Host defense peptides as new weapons in cancer treatment. *Cell. Mol. Life Sci. 62*, 784−790.

(6) Hoskin, D. W., and Ramamoorthy, A. (2008) Studies on anticancer activities of antimicrobial peptides. *Biochim. Biophys. Acta 1778*, 357−375.

(7) Matsuzaki, K., Sugishita, K., Fujii, N., and Miyajima, K. (1995) Molecular basis for membrane selectivity of an antimicrobial peptide, magainin 2. *Biochemistry 34*, 3423−3429.

(8) Matsuzaki, K. (2009) Control of cell selectivity of antimicrobial peptides. *Biochim. Biophys. Acta 1788*, 1687−1692.

(9) Utsugi, T., Schroit, A. J., Connor, J., Bucana, C. D., and Fidler, I. J. (1991) Elevated expression of phosphatidylserine in the outer membrane leaflet of human tumor cells and recognition by activated human blood monocytes. *Cancer Res. 51*, 3062−3066.

(10) Kleef, J., Ishiwata, T., Kumbasar, A., Friess, H., Büchler, M. W., Lander, A. D., and Korc, M. (1998) The cell-surface heparan sulfate proteoglycan glypican-1 regulates growth factor action in pancreatic carcinoma cells and is overexpressed in human pancreatic cancer. *J. Clin. Invest. 102*, 1662−1673.

(11) Burchell, J. M., Mungul, A., and Taylor-Papadimitriou, J. (2001) O-linked glycosylation in the mammary gland: Changes that occur during malignancy. *Journal of Mammary Gland Biology and Neoplasia 6*, 355−364.

(12) Papo, N., Seger, D., Makovitzki, A., Kalchenko, V., Eshhar, Z., Degani, H., and Shai, Y. (2006) Inhibition of tumor growth and elimination of multiple metastases in human prostate and breast xenografts by systemic inoculation if a host defense-like lytic peptide. *Cancer Res. 66*, 5371−5378.

(13) Matsuzaki, K., Murase, O., Tokuda, H., Funakoshi, S., Fujii, N., and Miyajima, K. (1994) Orientational and aggregational states of magainin 2 in phospholipid bilayers. *Biochemistry 33*, 3342−3349.

(14) Takeshima, K., Chikushi, A., Lee, K.-K., Yonehara, S., and Matsuzaki, K. (2003) Translocation of analogues of the antimicrobial peptides magainin and buforin across human cell membranes. *J. Biol. Chem. 278*, 1310−1315.

(15) Matsuzaki, K., Murase, O., Fujii, N., and Miyajima, K. (1996) An antimicrobial peptide, magainin 2, induced rapid flip-flop of phospholipids coupled with pore formation and peptide translocation. *Biochemistry 35*, 11361−11368.

(16) Yang, J. T., Wu, C.-S. C., and Martinez, H. M. (1986) Calculation of protein conformation from circular dichroism. *Methods Enzymol. 130*, 208−269.

(17) Bartlett, G. R. (1959) Phosphorus assay in column chromatography. *J. Biol. Chem. 234*, 466−468.

(18) Svennerholm, L. (1957) Quantitative estimation of sialic acids. II. A colorimetric resorcinol-hydrochloric acid method. *Biochim. Biophys. Acta 24*, 604−611.

(19) Yano, Y., Shimai, N., and Matsuzaki, K. (2010) Design of a soluble transmembrane helix for measurements of water-membrane partitioning. *J. Phys. Chem. B 114*, 1925−1931.

(20) Takakuwa, T., Konno, T., and Meguro, H. (1985) A new standard substance for calibration of circular dichroism: Ammonium *d*-10-camphorsulfonate. *Anal. Sci. 1*, 215−218.

(21) Lakowicz, J. R. (2006) *Principles of fluorecence specctroscopy*, 3rd ed., Springer, Singapore.

(22) Chattopadhyay, A., and London, E. (1987) Parallax method for direct measurement of membrane penetration depth utilizing fluorescence quenching by spin-labeled phospholipids. *Biochemistry 26*, 39−45.

(23) Lauer, S., Goldstein, B., Nolan, R. L., and Nolan, J. P. (2002) Analysis of cholera toxin−ganglioside interactions by flow cytometry. *Biochemistry 41*, 1742−1751.
(24) Yanagisawa, M., Ariga, T., and Yu, R. K. (2006) Fucosyl-GM1 expression and amyloid-β protein accumulation in PC12 cells. *J. Neurosci. Res. 84*, 1343−1349.
(25) Kakio, A., Nishimoto, S., Yanagisawa, K., Kozutsumi, Y., and Matsuzaki, K. (2001) Cholesterol-dependent formation of GM1 ganglioside-bound amyloid β-protein, an endogenous seed for Alzheimer amyloid. *J. Biol. Chem. 276*, 24985−24990.
(26) Chen, Y.-H., Yang, J. T., and Martinez, H. M. (1972) Determination of the secondary structures of proteins by circular dichroism and optical rotatory dispersion. *Biochemistry 11*, 4120−4131.
(27) Matsuzaki, K., Kato, K., and Yanagisawa, K. (2010) Aβ polymerization through interaction with membrane gangliosides. *Biochim. Biophys. Acta 1801*, 868−877.
(28) Lee, H. S., Park, C. B., Kim, J. M., Jang, S. A., Park, I. Y., Kim, M. S., Cho, J. H., and Kim, S. C. (2008) Mechanism of anticancer activity of buforin IIb, a histone H2A-derived peptide. *Cancer Lett. 271*, 47−55.
(29) Wenk, M. R., and Seelig, J. (1998) Magainin 2 amide interaction with lipid membranes: Calorimetric detection of peptide binding and pore formation. *Biochemistry 37*, 3909−3916.
(30) Wieprecht, T., Beyermann, M., and Seelig, J. (1999) Binding of antibacterial magainin peptides to electrically neutral membranes: Thermodynamics and structure. *Biochemistry 38*, 10377−10387.
(31) Matsuzaki, K., Harada, M., Handa, T., Funakoshi, S., Fujii, N., Yajima, H., and Miyajima, K. (1989) Magainin 1-induced leakage of entrapped calcein out of negatively-charged lipid vesicles. *Biochim. Biophys. Acta 981*, 130−134.
(32) Wolber, P. K., and Hudson, B. S. (1979) An analytical solution to the Förster energy transfer problem in two dimensions. *Biophys. J. 28*, 197−210.
(33) Beschiaschvili, G., and Seelig, J. (1990) Melittin binding to mixed phosphatidylglycerol/phosphatidylcholine membranes. *Biochemistry 29*, 52−58.
(34) Eisenberg, M., Gresalfi, T., Riccio, T., and McLaughlin, S. (1979) Adsorption of monovalent cations to bilayer membranes containing negative phospholipids. *Biochemistry 18*, 5213−5223.
(35) Imura, Y., Nishida, M., and Matsuzaki, K. (2007) Action mechanism of PEGylated magainin 2 analogue peptide. *Biochim. Biophys. Acta 1768*, 2578−2585.
(36) Lee, M.-T., Chen, F.-Y., and Huang, H. W. (2004) Energetics of pore formation induced by membrane active peptides. *Biochemistry 43*, 3590−3599.
(37) Ludtke, S. J., He, K., and Huang, H. (1995) Membrane thinning caused by magainin 2. *Biochemistry 34*, 16764−16769.